ARGONNE NATIONAL LABORATORY
9700 South Cass Avenue
Argonne, Illinois 60439

THE MINPACK-2 TEST PROBLEM COLLECTION (PRELIMINARY VERSION)

Brett M. Averick[†], Richard G. Carter[†], and Jorge J. Moré

Mathematics and Computer Science Division

Technical Memorandum No. 150

May 1991

Work supported in part by the Applied Mathematical Sciences subprogram of the Office of Energy Research, U.S. Department of Energy, under Contract W-31-109-Eng-38

[†] Army High Performance Computing Research Center (AHPCRC), Institute of Technology, University of Minnesota, 1100 Washington Avenue South, Minneapolis, Minnesota 55415

ABSTRACT

The Army High Performance Computing Research Center at the University of Minnesota and the Mathematics and Computer Science Division at Argonne National Laboratory are collaborating on the development of the software package MINPACK-2. As part of the MINPACK-2 project we are developing a collection of significant optimization problems to serve as test problems for the package. This report describes the problems in the preliminary version of this collection.

1 Introduction

The Army High Performance Computing Research Center at the University of Minnesota and the Mathematics and Computer Science Division at Argonne National Laboratory have initiated a collaboration for the development of the software package MINPACK-2. As part of the MINPACK-2 project, we are developing a collection of significant optimization problems to serve as test problems for the package. This report describes some of the problems in the preliminary version of this collection.

Optimization software has often been developed without any specific application in mind. This generic approach has worked well in many cases, but as we seek the solution of larger and more complex optimization problems on high-performance computers, the development of optimization software should take into account specific optimization problems that arise in a wide range of applications. This observation was the motivation for the main requirement for inclusion in this collection: each problem must come from a real application and be representative of other commonly encountered problems. Problems in the preliminary version of the collection come from such diverse fields as fluid dynamics, medicine, combustion, nondestructive testing, chemical kinetics, lubrication, mathematics, and superconductivity.

Our interest in high-performance computers was the reason for the second requirement for inclusion in this collection: each application selected must lead to a large-scale optimization problem. Many of the problems in the preliminary version of the collection are finite dimensional approximations to problems that are naturally expressed in an infinite dimensional setting. Thus, the solution of these problems usually requires the solution of an optimization problem with a large number of variables.

We have also included in this collection small dimensional application problems with interesting features. In particular, we have included difficult problems that are of especial use in testing the robustness of an optimization algorithm. Although such problems may not be large-scale with respect to problem dimension, they can be computationally intensive and difficult to parallelize.

The optimization problems in this collection are divided into three broad categories: systems of nonlinear equations, nonlinear least squares, and general minimization problems. Most of the problems in the preliminary version of the collection either are unconstrained or have only upper and lower bounds on the variables. We are also interested in large-scale optimization problems with more general constraints, but our initial efforts have focused on bound constrained problems, in view of our current work in developing software to solve these problems.

The effort needed to develop a large-scale problem for this collection can be considerable. Inclusion of a problem in the collection requires code for the evaluation of the functions associated with the application, and verification that the code actually represents

the specified application. Our experience in developing these problems has shown that the verification process is important, because in several cases this process has unveiled errors in the description of the application. We have tried to minimize the effort needed to include a problem in this collection by concentrating on generic applications that can be described (at least superficially) in two pages.

We also emphasize that we are developing code for the evaluation of the functions and the associated derivatives in Fortran 77 to enhance portability. This is an important part of our effort. There are several collections of interesting optimization problems, but in many cases software for these problems is either not available or is available in a restricted format.

The primary purpose of this collection is to provide difficult test cases for MINPACK-2. We are interested in examining the following issues:

How robust is the software with respect to poor initial approximations?

How does the software perform on badly scaled problems?

How robust is the code with respect to noise in the user-supplied software?

How does the software perform on large-scale problems?

How does the software perform on diverse vector and parallel architectures?

A complete discussion of these issues is not in the scope of this paper, but we mention that with these problems it is entirely appropriate to use computing time as a measure of efficiency: the computational expense (as measured by the number of floating-point operations) of evaluating the functions in this collection is relatively small, roughly the same order as the number of variables in the problem. For optimization software designed for cases in which the expense of the user-supplied software is dominant, these same test problems can be used to evaluate the software by using the number of calls to the user-supplied software as a measure of efficiency.

In the remainder of this paper we describe the problems in this collection. We have not attempted to provide a detailed description of the applications. The emphasis of this paper is on the mathematical formulation of the application as an optimization problem. We provide background information on the application; details that are not needed to understand the formulation of the application have been omitted. For example, we do not usually specify the standard starting point x_s in the optimization problem. Our intention is to provide these details at a later date.

2 Systems of Nonlinear Equations

The solution to a system of nonlinear equations specified by a mapping $f : \Re^n \to \Re^n$ is a vector $x \in \Re^n$ such that $f(x) = 0$. Algorithms for systems of nonlinear equations usually approach this problem by seeking a local minimizer to the problem

$$\min\{\|f(x)\| : x_l \le x \le x_u\},$$

where x_l and x_u are bounds on the solution x, and $\|\cdot\|$ is some norm on $\Re^n$. Most algorithms use the l_2 norm. Interestingly enough, codes for systems of nonlinear equations do not tend to have provisions for handling bounds (or more general constraints) on the variables.

2.1 Flow in a Channel

The problem of fluid injection through one side of a long vertical channel leads to the boundary value problem

$$u'''' = R[u'u'' - uu'''], \qquad 0 \le t \le 1,$$

$$u(0) = u'(0) = 0, \quad u(1) = 1, \quad u'(1) = 0,$$

where u is the potential function, u' is the tangential velocity of the fluid, and R is the Reynolds number. This problem is interesting because it is easy to solve for small Reynolds numbers but becomes increasingly difficult to solve as R increases.

This problem was formulated by Huang [12]. In our formulation we have followed Ascher, Mattheij, and Russell [2, p. 7].

We solve this nonlinear boundary value problem by a k-stage collocation method. Consider the general boundary value problem

$$u^{(m)}(t) = F(t, u(t), u'(t), \cdots, u^{(m-1)}(t)), \qquad t \in (a, b),$$

with m total boundary conditions given at $t = a$ and $t = b$, and let

$$a = t_1 < t_2 < \cdots < t_{n_0} < t_{n_0+1} = b$$

be a partitioning of $[a, b]$, with $h_i = t_{i+1} - t_i$. A k-stage collocation method is defined in terms of k points

$$0 < \rho_1 < \rho_2 < \cdots < \rho_k < 1.$$

We choose the collocation points ρ_i as the roots of the Legendre polynomial of order $k \ge m$. This choice guarantees that superconvergence occurs at the mesh points t_i. The k-stage collocation method approximates the solution to the boundary value problem by a piecewise polynomial u_π, where u_π is a polynomial of order $m + k$ in each subinterval $[t_i, t_{i+1}]$. Thus,

u_π is defined in terms of $n_0(m+k)$ parameters. We specify these parameters by requiring that $u_\pi \in C^{m-1}[a,b]$, that u_π satisfy the m given boundary conditions, and that u_π satisfy the differential equation at the collocation points

$$\xi_{ij} = t_i + h_i \rho_j, \qquad 1 \le i \le n_0, \quad 1 \le j \le k.$$

The piecewise polynomial approximation u_π in the interval $[t_i, t_{i+1}]$ is of the form

$$\sum_{j=1}^{m} \frac{(t-t_i)^{j-1}}{(j-1)!} v_{ij} + h_i^m \sum_{j=1}^{k} \phi_j\left(\frac{t-t_i}{h_i}\right) w_{ij}, \qquad 1 \le i \le n_0,$$

where we choose the basis representation (Ascher, Mattheij, and Russell [2, pp. 247–249])

$$\phi_j(t) = \frac{t^{m+j-1}}{(m+j-1)!}, \qquad 1 \le j \le k.$$

A simple computation shows that in this representation

$$v_{ij} = u_\pi^{(j-1)}(t_i), \qquad 1 \le i \le n_0, \quad 1 \le j \le m,$$

and that

$$w_{ij} = h_i^{j-1} u_\pi^{(m+j-1)}(t_i), \qquad 1 \le i \le n_0, \quad 1 \le j \le k.$$

Thus, bounds on a derivative of u_π at t_i can be specified by bounding v_{ij} or w_{ij}.

We guarantee that $u_\pi \in C^{m-1}[a,b]$ by enforcing continuity at the interior grid points. The continuity equations are thus given by

$$u_\pi^{(l-1)}(t_i^-) = u_\pi^{(l-1)}(t_i^+), \qquad 1 \le l \le m, \quad 1 < i \le n_0.$$

The collocation equations are then

$$u_\pi^{(m)}(\xi_{ij}) = F(\xi_{ij}, u_\pi(\xi_{ij}), u_\pi'(\xi_{ij}), \ldots, u_\pi^{(m-1)}(\xi_{ij})), \qquad 1 \le j \le k, \quad 1 \le i \le n_0.$$

These equations, together with the m boundary conditions, lead to a system of $n_0(m+k)$ equations in the $n_0(m+k)$ unknowns v_{ij} and w_{ij}.

We choose $k = 4$ and $n_0 = 40$ in our numerical results. This choice leads to a system of nonlinear equations with 320 variables. A plot of the computed tangential velocity u' for several values of R appears in Figure 2.1; similar results were obtained by Ascher [1] with $k = 5$. Note, in particular, the steep gradient near $t = 0$ as R increases.

The three plots in Figure 2.1 were generated by solving a sequence of five problems with $R_0 = 0$, $R_1 = 10^2$, $R_2 = 10^3$, $R_3 = \frac{1}{2}10^4$, and $R_4 = 10^4$. The problem with $R_0 = 0$ is linear; its solution is used as the initial approximation to the problem for R_1. The continuation process continues in this manner, with the initial approximation to the problem for R_{i+1} being the solution to the problem for R_i. The whole continuation process requires 26 function evaluations. An interesting observation is that with the continuation process we were able to obtain the solution for $R = 10^4$, but this solution was not obtainable if we started from the solution for $R = 0$.

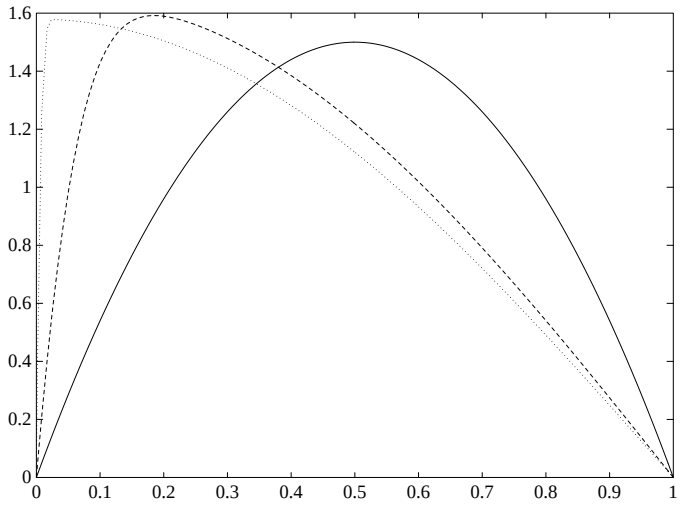

Figure 2.1: Tangential velocity u' for $R = 0, 10^2, 10^4$ (solid, dashed, dotted)

2.2 Swirling Flow

The steady flow of a viscous, incompressible, axisymmetric fluid between two rotating, infinite coaxial disks, located at $t = 0$ and $t = 1$, yields the boundary value problem

$$\epsilon f'''' + ff''' + gg' = 0, \quad \epsilon g'' + fg' + f'g = 0, \qquad 0 \le t \le 1,$$

$$f(0) = f'(0) = f(1) = f'(1) = 0, \quad g(0) = \Omega_0, \quad g(1) = \Omega_1$$

where f' is radial velocity, g is angular velocity (Ω_0 and Ω_1 are the angular velocities of the infinite disks), and $0 \le \epsilon \ll 1$ is a viscosity parameter. This problem is interesting since it is easy to solve for ϵ close to 1 but becomes increasingly difficult to solve as ϵ decreases. In our formulation we have followed Parter [24]. (We note that there is a typographical error in the formulation of Ascher, Mattheij, and Russell [2, p. 23]; in this reference the first equation is $\epsilon f'''' + f''' + g' = 0$.)

The swirling flow problem is described by a (coupled) system of boundary value problems. Systems of this type can be solved by a natural extension of the k-stage collocation method discussed above. A k-stage collocation method approximates the solution to a system of p boundary value problems by a vector-valued function $u_\pi : [a, b] \to \Re^p$, where the j-th component of u_π is a polynomial of order $m_j + k$ in each subinterval $[t_i, t_{i+1}]$, and m_j is the degree of the j-th boundary value problem. Thus u_π is defined in terms of $n_0(pk + m_0)$ parameters, where m_0 is the sum of all the degrees. In many cases all the boundary value problems have the same degree (for example, in initial value problems), and then u_π is defined in terms of $n_0 p(k + m)$ parameters, where m is the common degree.

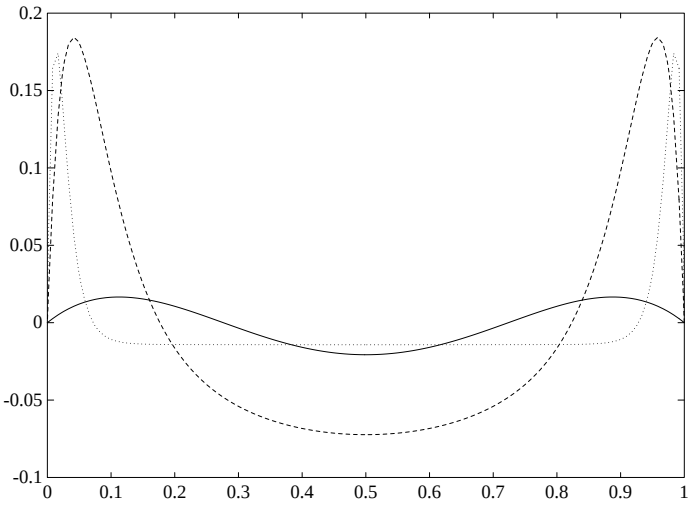

Figure 2.2: Radial velocity f' for $\epsilon = 10^{-1}, 10^{-3}, 10^{-4}$ (solid, dashed, dotted)

The parameters that define u_π are determined by the continuity and collocation equations for each boundary value problem, together with the m_0 boundary conditions. If all the boundary value problem have the same degree, the continuity equations are

$$u_\pi^{(l-1)}(t_i^-) = u_\pi^{(l-1)}(t_i^+), \qquad 1 \le l \le m, \quad 1 < i \le n_0.$$

Note that in this case these are vector equations. Similarly, the collocation equations are

$$u_\pi^{(m)}(\xi_{ij}) = F(\xi_{ij}, u_\pi(\xi_{ij}), u'_\pi(\xi_{ij}), \ldots, u_\pi^{(m-1)}(\xi_{ij})), \qquad 1 \le j \le k, \quad 1 \le i \le n_0.$$

If the boundary value problems have different degrees (as in the swirling flow problem), then these equations have to be modified in an obvious manner since m depends on the component of F.

For the swirling flow problem, $p = 2$ and $m_0 = 6$. For our numerical results, we choose $k = 4$ and $n_0 = 40$. This leads to a system of nonlinear equations with 560 variables. The plots of the computed radial velocity f' and the computed angular velocity g appear in Figures 2.2 and 2.3, respectively. In these plots, $\Omega_0 = -1$ and $\Omega_1 = 1$. For these values of Ω_0 and Ω_1, McLeod and Parter [16] have shown that there is a solution to the swirling flow problem such that the functions f and g are odd functions about $t = \frac{1}{2}$, the function g is strictly monotone on $(0, \frac{1}{2})$, and there is a t_1 in $(0, \frac{1}{2})$ with $f'(t) > 0$ on $(0, t_1)$ and $f'(t) < 0$ on $(t_1, \frac{1}{2})$. These results are confirmed by the plots.

Continuation was used to solve these problems with $\epsilon_1 = 10^{-1}$, $\epsilon_2 = 10^{-3}$, and $\epsilon_3 = 10^{-4}$. The initial approximation to the problem with $\epsilon_1 = 10^{-1}$ was the solution of the boundary value problem with $\epsilon = \infty$. The continuation process required 24 function evaluations.

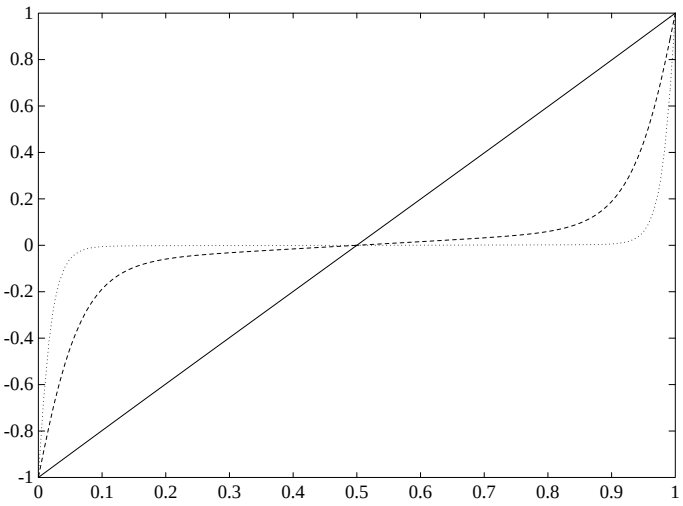

Figure 2.3: Angular velocity g for $\epsilon = 10^{-1}, 10^{-3}, 10^{-4}$ (solid, dashed, dotted)

2.3 The Human Heart Dipole

The human heart dipole problem arises in the experimental electrolytic determination of the resultant dipole moment in the human heart. The problem is of the form

$$f_1(x) = x_1 + x_2 - \sigma_{mx}$$
$$f_2(x) = x_3 + x_4 - \sigma_{my}$$
$$f_3(x) = x_5 x_1 + x_6 x_2 - x_7 x_3 - x_8 x_4 - \sigma_A$$
$$f_4(x) = x_7 x_1 + x_8 x_2 + x_5 x_3 + x_6 x_4 - \sigma_B$$
$$f_5(x) = x_1(x_5^2 - x_7^2) - 2x_3 x_5 x_7 + x_2(x_6^2 - x_8^2) - 2x_4 x_6 x_8 - \sigma_C$$
$$f_6(x) = x_3(x_5^2 - x_7^2) + 2x_1 x_5 x_7 + x_4(x_6^2 - x_8^2) + 2x_2 x_6 x_8 - \sigma_D$$
$$f_7(x) = x_1 x_5(x_5^2 - 3x_7^2) + x_3 x_7(x_7^2 - 3x_5^2) + x_2 x_6(x_6^2 - 3x_8^2) + x_4 x_8(x_8^2 - 3x_6^2) - \sigma_E$$
$$f_8(x) = x_3 x_5(x_5^2 - 3x_7^2) - x_1 x_7(x_7^2 - 3x_5^2) + x_4 x_6(x_6^2 - 3x_8^2) - x_2 x_8(x_8^2 - 3x_6^2) - \sigma_F$$

with data $\sigma_{mx}, \sigma_{my}, \sigma_A, \sigma_B, \sigma_C, \sigma_D, \sigma_E, \sigma_F$. In this problem $n = 8$.

This problem was formulated by Nelson and Hodgkin [20]. In our formulation we have followed Dennis, Gay, and Vu [6]. They also propose a six-variable version of this problem, obtained by using the first two equations to eliminate two of the first four variables. We have not implemented this reduced problem.

There are five versions of the eight-variable problem depending on the data and the starting point. The last three versions can be difficult to solve, even from the standard starting point.

An interesting aspect of this problem is that the system is unchanged if the variables are permuted according to the

$$(1,2,3,4,5,6,7,8) \rightarrow (2,1,4,3,6,5,8,7)$$

permutation. This implies that solutions appear in pairs. In all of these problems, we have only found one pair of solutions. If a unique solution is desired, the bound $x_1 \leq 0$ can be imposed. There are no natural bounds associated with this problem, but the components of the solution lie in the interval $[-20, 20]$.

2.4 Combustion of Propane

This chemical equilibrium problem describes the combustion of propane in air. Each unknown represents the number of moles of a given product formed for each mole of propane; ten products are considered in this reaction. The problem is of the form

$$\begin{aligned}
f_1(x) &= x_1 + x_4 - 3 \\
f_2(x) &= 2x_1 + x_2 + x_4 + x_7 + x_8 + x_9 + 2x_{10} - R \\
f_3(x) &= 2x_2 + 2x_5 + x_6 + x_7 - 8 \\
f_4(x) &= 2x_3 + x_9 - 4R \\
f_5(x) &= K_5 x_2 x_4 - x_1 x_5 \\
f_6(x) &= K_6 x_2^{1/2} x_4^{1/2} - x_1^{1/2} x_6 \left(\frac{p}{x_{11}}\right)^{1/2} \\
f_7(x) &= K_7 x_1^{1/2} x_2^{1/2} - x_4^{1/2} x_7 \left(\frac{p}{x_{11}}\right)^{1/2} \\
f_8(x) &= K_8 x_1 - x_4 x_8 \left(\frac{p}{x_{11}}\right) \\
f_9(x) &= K_9 x_1 x_3^{1/2} - x_4 x_9 \left(\frac{p}{x_{11}}\right)^{1/2} \\
f_{10}(x) &= K_{10} x_1^2 - x_4^2 x_{10} \left(\frac{p}{x_{11}}\right) \\
f_{11}(x) &= x_{11} - \textstyle\sum_{j=1}^{10} x_j,
\end{aligned}$$

with data $K_5, \ldots, K_{10}$, and parameters p and R. The parameter p is the pressure in atmospheres and R expresses the relative amounts of air and fuel. In this problem $n = 11$, $p = 40$, and $R = 10$. In our formulation of this problem we have followed Meintjes and Morgan [17].

This problem may be difficult to solve because of the presence of square roots in the function components and the possibility of generating an iterate with a negative component.

There are no difficulties in solving this problem from the standard starting point x_s, but an unconstrained algorithm is likely to generate an iterate with a negative component from the starting point $10x_s$. The bounds $x_j \geq 0$ can be used to solve this problem.

2.5 Combustion of Propane – Reduced Formulation

This chemical equilibrium problem, like the preceding one, describes the combustion of propane in air. This formulation, however, uses the element variables of Meintjes and Morgan [17] to avoid the square roots in the function evaluations. The formulation of the problem in terms of element variables also reduces the problem to a system of the form

$$
\begin{aligned}
f_1(x) &= x_1x_2 + x_1 - 3x_5 \\
f_2(x) &= 2x_1x_2 + x_1 + 2R_{10}x_2^2 + x_2x_3^2 + R_7x_2x_3 + R_9x_2x_4 + R_8x_2 - Rx_5 \\
f_3(x) &= 2x_2x_3^2 + R_7x_2x_3 + 2R_5x_3^2 + R_6x_3 - 8x_5 \\
f_4(x) &= R_9x_2x_4 + 2x_4^2 - 4Rx_5 \\
f_5(x) &= x_1x_2 + x_1 + R_{10}x_2^2 + x_2x_3^2 + R_7x_2x_3 + R_9x_2x_4 + R_8x_2 + R_5x_3^2 + R_6x_3 + x_4^2 - 1
\end{aligned}
$$

with data $R_5, \ldots, R_{10}$ which depends on the parameters p and R described previously. In this problem $n = 5$, $p = 40$, and $R = 10$. (We note that there is a typographical error in the paper of Meintjes and Morgan [17]; the last term in the equation defining f_4 should be $-4Rx_5$ and not $+4Rx_5$.)

This system of equations has four solutions with real components for $p = 40$ and $R = 10$. There is only one solution with all positive components; this is the desired solution to the physical problem.

This problem is not difficult to solve, but unless bounds are imposed, the physical solution may not be found. An unconstrained algorithm usually finds the physical solution from the standard starting point x_s but tends to converges to non-physical solutions from the starting points $10x_s$ and $100x_s$. The bounds $x_j \geq 0$ can be used to obtain the physical solution.

3 Least Squares Problems

Solutions to a nonlinear least squares problem subject to equality and inequality constraints are local minimizers of the problem

$$\min\{\|f(x)\|_2^2 : c_l \leq c(x) \leq c_u\},$$

where $f : \Re^n \to \Re^m$ defines the residuals of the least squares problem, $c : \Re^n \to \Re^p$ is the constraint function, and c_l and c_u are bounds. Equality constraints are obtained when components of c_l and c_u have the same value. Problems in this section include bound-constrained problems where $c(x) = x$, and equality constrained problems where $c_l = c_u$.

3.1 Isomerization of α-pinene – Direct Formulation

This problem requires the determination of the reaction coefficients in the thermal isomerization of α-pinene. The linear kinetic model proposed for this problem is of the form

$$\begin{aligned} y_1' &= -(\theta_1 + \theta_2)y_1 \\ y_2' &= \theta_1 y_1 \\ y_3' &= \theta_2 y_1 - (\theta_3 + \theta_4)y_3 + \theta_5 y_5 \\ y_4' &= \theta_3 y_3 \\ y_5' &= \theta_4 y_3 - \theta_5 y_5 \end{aligned} \tag{3.1}$$

where $\theta_1, \ldots, \theta_5$ are the unknown coefficients. Initial conditions for the differential equation are known. In this problem the relative concentrations of α-pinene and three by-products are measured at eight time points, while the relative concentration of a fourth by-product is derived from the other concentrations. Thus, at a set of eight time points $\tau_1, \ldots, \tau_8$, vectors of concentration measurements z_j are given for y at τ_j, where y is the solution to the system of differential equations which governs the reaction. The α-pinene problem is to minimize

$$\sum_{j=1}^{8} \|y(\tau_j; \theta) - z_j\|^2, \tag{3.2}$$

where θ is the vector with components $\theta_1, \ldots, \theta_5$ of unknown reaction coefficients. This formulation of the α-pinene problem is based on the work of Box, Hunter, MacGregor, and Erjavac [3].

The α-pinene problem is a typical example of inverse problems involving differential equations that arise in chemical kinetics. In the general case the reaction is governed by a system of p differential equations

$$y'(t) = F(t, y(t), \theta), \qquad a \leq t \leq b,$$

which depend on a vector $\theta \in \Re^q$ of unknown parameters. Initial conditions for $y \in \Re^p$ may also be provided, and may also depend on θ. In the α-pinene problem $p = q$ and F is bilinear in θ and y, but these conditions do not hold in general.

We formulate the α-pinene problem as an unconstrained nonlinear least squares problem involving a numerical approximation $u(t;\theta)$ to $y(t;\theta)$ obtained from a fourth-order Runge-Kutta scheme over n_0 time intervals. The optimization problem is then to determine a parameter vector $\theta \in \Re^5$ that solves the problem

$$\min \left\{ \sum_{j=1}^{8} \|u(\tau_j;\theta) - z_j\|^2 : \ \theta_i \geq 0, \ i = 1, \ldots, 5 \right\}. \tag{3.3}$$

This is a nonlinear least squares problem with $m = 40$ equations and $n = 5$ variables. The constraints $\theta_i \geq 0$ arise from physical considerations. For sufficiently large n_0, we expect that solutions to problem (3.3) will be close to a solution of problem (3.2).

An approximation to the Jacobian matrix for this formulation of the α-pinene problem can be obtained by solving a system of coupled ordinary differential equations consisting of the original α-pinene equations and 25 additional equations. The additional equations are obtained by differentiating each of the α-pinene equations (3.1) by θ_j for $j = 1, \ldots, 5$, and noting that if

$$w_{i,j}(\tau;\theta) \equiv \partial_{\theta_j} y_i(\tau;\theta),$$

then

$$w'_{i,j}(\tau;\theta) = \partial_{\theta_j} y'_i(\tau;\theta).$$

The approximation to the Jacobian matrix obtained by this method is more accurate than an approximation based on differences of function values.

In our numerical results we used a Runge-Kutta method with $n_0 = 80$ time intervals. The solution of this version of the α-pinene problem is not difficult to obtain from the standard start θ_s, but becomes increasingly difficult to solve from remote starting points. The approximation $u(t,\cdot)$ for the optimal θ, shown in Figure 3.1, is an excellent fit to the data.

Numerical difficulties in solving this version of the α-pinene problem are mainly due to the result that with fixed-steplength Runge-Kutta techniques and sufficiently large values of θ, the approximation $u(t;\theta)$ becomes unbounded as t increases. In contrast, the true solution $y(t;\theta)$ of the differential equations problem remains bounded for $t \geq 0$ for any nonnegative choice of $\theta_1, \ldots, \theta_5$. Hence, our test problem becomes difficult to solve given poor initial estimates for θ. We illustrate this remark by noting that while the initial residual norm computed at the standard starting point was 7.03, the residual computed at 50 times this starting point was 7.22×10^{110}. Hence, this problem is quite challenging with respect to choice of initial estimates.

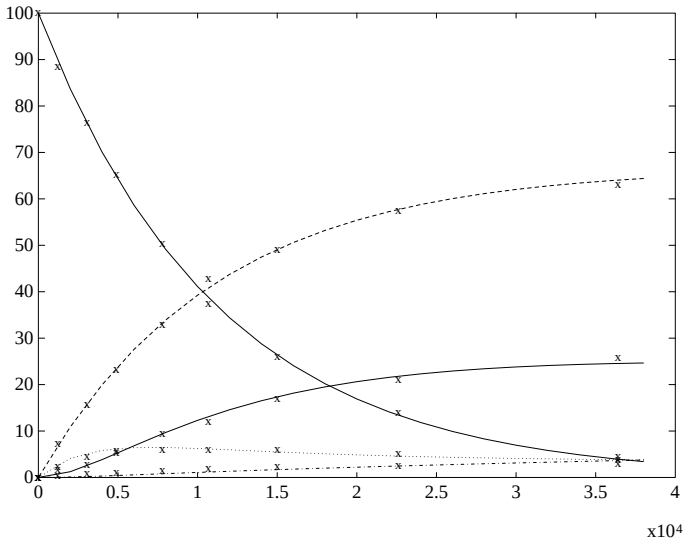

Figure 3.1: The five components of $u(t, \theta)$ for the α-pinene problem with the optimal θ

In general, extreme sensitivity to initial θ estimates is a hallmark of problems of this type. As with the α-pinene example, integration may be done using a fixed-steplength numerical solver of initial value problems. Decreasing the steplength does not affect the size of the optimization problem and may enlarge the set of possible θ for which the solver is stable, but of course adds to the computational expense of residual and Jacobian evaluations. A more interesting approach is to use an adaptive solver, which automatically adjusts steplengths to correspond to the level of accuracy requested by the user, and can be expected to be more stable than fixed steplength solvers. The resultant approximation $u(t; \theta)$ may not be smooth with respect to small variations in θ (Lyness [15] provides an interesting discussion of this point), but this approach allows the possibility of using optimization software that makes use of variable-accuracy evaluations to avoid the expense of full accuracy solutions whenever possible. This challenging category of test problems has been neglected in the literature.

3.2 Isomerization of α-pinene – Collocation Formulation

The second α-pinene problem requires the determination of the reaction coefficients in the thermal isomerization of α-pinene; in this problem, however, collocation is used to approximate the solution of the differential equations that define the kinetics of the problem. This formulation of the α-pinene problem is based on the work of Tjoa and Biegler [25].

The collocation method for initial value problems is a special case of the collocation method for boundary value problems that was used in Sections 2.1 and 2.2. Recall that the

k-stage collocation method is defined in terms of a partition

$$a = t_1 < t_2 < \cdots < t_{n_0} < t_{n_0+1} = b$$

of $[a,b]$, and a set of k collocation points in each interval $[t_i, t_{i+1}]$. The collocation method approximates the solution of the system of differential equations by a vector-valued function $u_\pi : [a,b] \rightarrow \Re^p$, where each component of u_π is a polynomial of order $k+1$ in each subinterval $[t_i, t_{i+1}]$. Thus u_π is defined in terms of $n_0 p(k+1)$ parameters. In the collocation formulation these parameters are determined by requiring that $u_\pi \in C[a,b]$ and that u_π satisfy the differential equation at the collocation points. In the usual case we are given p initial values; these initial values together with the continuity and collocation equations lead to a system of $n_0 p(k+1)$ equations in the $n_0 p(k+1)$ parameters that define u_π.

We now formulate the α-pinene problem as a minimization problem subject to equality constraints. Let $x \in \Re^n$ be the vector that defines u_π, with $n = n_0 p(k+1)$. We define $u_\pi(\tau; x) \equiv u_\pi(\tau)$ to make explicit the dependence of u_π on x. If we write the initial value, continuity, and collocation equations as constraints of the form

$$c(x, \theta) = 0,$$

where $c : \Re^{n+q} \rightarrow \Re^n$, then the optimization problem is

$$\min \left\{ \sum_{j=1}^{m} \| u_\pi(\tau_j; x) - z_j \|^2 : c(x, \theta) = 0 \right\}.$$

The l_2 penalty approach to the solution of this problem leads to a least squares problem of the form

$$\min \left\{ \sum_{j=1}^{m} \| u_\pi(\tau_j; x) - z_j \|^2 + \tfrac{1}{2} \sum_{i=1}^{n} \sigma_i c_i(x, \theta)^2 \right\},$$

where $\sigma_i > 0$, while the augmented Lagrangian approach leads to a problem of the form

$$\min \left\{ \sum_{j=1}^{m} \| u_\pi(\tau_j; x) - z_j \|^2 + \tfrac{1}{2} \sum_{i=1}^{n} \sigma_i \left[c_i(x, \theta) + \frac{\lambda_i}{\sigma_i} \right]^2 \right\},$$

where $\sigma_i > 0$ and $\lambda_i \in \Re$ is an estimate of the Lagrange multiplier for the constraint c_i. Both approaches lead to least squares problem with $mp + n$ equations and $n + q$ variables. Recall that $n = n_0 p(k+1)$ and that n_0 is the number of subintervals, $k+1$ is the order of the polynomials that define u_π in each subinterval, p is the number of differential equations in the model, q is the number of components in the parameter vector θ, and m is the number of data points. Note that n_0 and k can be specified, while the other parameters are dependent on the problem. Arbitrarily large-dimensional test problems can be generated by selecting larger values of n_0.

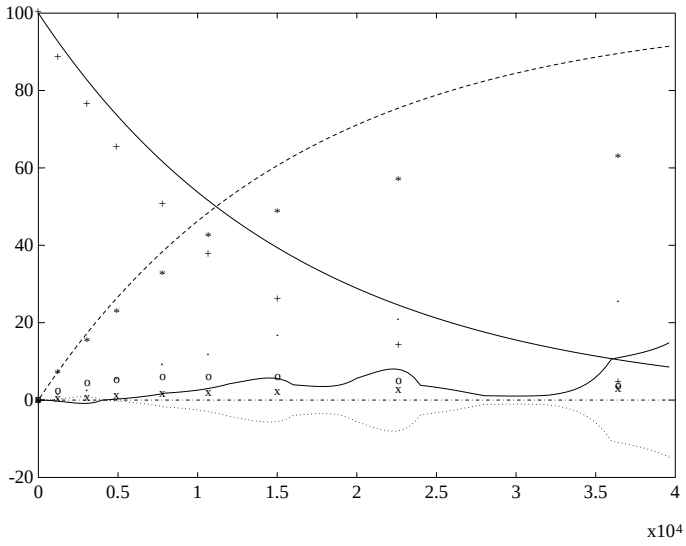

Figure 3.2: Spurious solution $u(t;\theta)$ to the α-pinene problem

For the α-pinene problem, $p = q = 5$, and $m = 8$. We selected $k = 4$ and $n_0 = 10$, so our least squares problem has 290 equations and 255 variables. Convergence from the standard starting point is not difficult. The final approximation obtained for y was identical to that shown in Figure 3.1.

The collocation approach demonstrates the value of using simple constraints on the variables to enforce the known nonnegativity of the components of θ. For sufficiently remote starting points, unconstrained least squares algorithms applied to this problem may converge to a different local minimizer with some components of θ negative, with u as shown in Figure 3.2. A bound version would not have encountered this spurious local solution. Simple bound constraints on the variables defining the approximation u_π can also be used to enforce $u_\pi(t_j) \geq 0$ at the node points t_j — a desirable feature in chemical engineering problems where negative concentrations have no physical meaning. Similarly, if physical considerations dictate that a given component of u_π be increasing or decreasing, simple constraints on the variables can ensure that a given component of $u'_\pi(t_j)$ is of the correct sign. These capabilities for constraining u are not present in the direct approach.

3.3 Coating Thickness Standardization

The coating thickness problem arises from the need to nondestructively determine any nonuniformity in the lead-tin coating on samples of standard reference materials. This is a multiple-response data-fitting problem communicated by Janet Rogers of the National Institute of Standards and Technology.

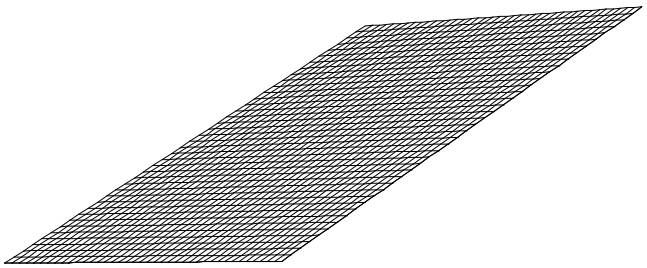

Figure 3.3: Coating thickness standards model $z_1(\xi_1, \xi_2)$ for optimal $x_1, \ldots, x_4$

At each of n_0 isolated points on the surface, we have measurements y_i for the coating thickness, the relative abundance y_{i+n_0} of lead to tin, and the surface coordinates $(\xi_1, \xi_2)_i$ at which the measurements were made. All four of these values are subject to error. We model the thickness of the coating and the relative abundance of tin to lead using simple bilinear tensor-product functions

$$\begin{aligned} z_1(\xi_1, \xi_2) &= x_1 + x_2\xi_1 + x_3\xi_2 + x_4\xi_1\xi_2, \\ z_2(\xi_1, \xi_2) &= x_5 + x_6\xi_1 + x_7\xi_2 + x_8\xi_1\xi_2. \end{aligned}$$

We seek values of the parameters $x_1, \ldots, x_8$, and small perturbations $x_9, \ldots, x_{8+2n_0}$ to the measured coordinates $(\xi_1, \xi_2)_i$ which fit the data in a least squares sense. This formulation leads to a least squares problem with residuals of the form

$$\begin{aligned} f_i(x) &= z_1(\xi_{1,i} + x_{8+i}\,,\, \xi_{2,i} + x_{8+i+n_0}) - y_i, \qquad 1 \le i \le n_0, \\ f_{i+n_0}(x) &= z_2(\xi_{1,i} + x_{8+i}\,,\, \xi_{2,i} + x_{8+i+n_0}) - y_{i+n_0}, \qquad 1 \le i \le n_0, \end{aligned}$$

and

$$f_{i+2n_0}(x) = w_i\, x_{8+i}, \qquad 1 \le i \le 2n_0,$$

where y_i and $\xi_{1,i}$, $\xi_{2,i}$ are the measured data and w_i is a set of weights. These residuals define a least squares problem with $n = 8 + 2n_0$ variables and $m = 4n_0$ equations. In the data supplied by Susannah Shiller of the National Institute of Standards and Technology, $n_0 = 63$, so that $n = 134$ and $m = 252$.

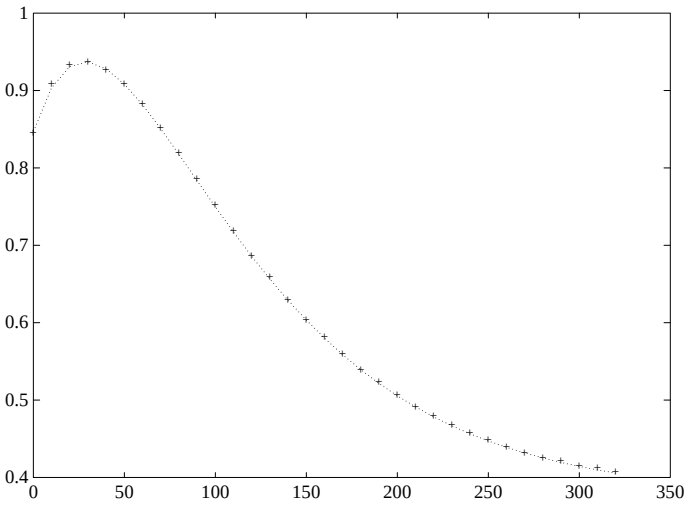

Figure 3.4: Exponential data fitting problem I

This problem is not difficult to solve from any of the starting values. Convergence always takes place to the same minimizer. At the solution x^* we have

$$\|f(x^*)\| = 0.7109842,$$

which reveals an excellent fit of the model to the data, since y_i is of order 10.

A plot of the model z_1 as a function of (ξ_1, ξ_2), with $x_1, \ldots, x_4$ set to the optimal values for the parameters, appears in Figure 3.3. This plot suggests that the model is almost linear in the region of interest. However, the relationship is not *exactly* linear because a calculation shows that in this region the first component of the gradient of the model varies over the interval $[16.4, 18.6]$, while the second component varies over the interval $[1.17, 1.33]$.

We have omitted a plot of the model z_2 with optimal $x_5, \ldots, x_8$ because the plot is similar. Moreover, for this model we also conclude that the relationship between the model and the independent parameters is almost linear in the region of interest.

3.4 Exponential Data Fitting I

This is an exponential data fitting problem using data supplied by A. M. Sargeson from the Research School of Chemistry of the Australian National University. The problem is of the form

$$f_i(x) = y_i - \Big(x_1 + x_2 \exp(-t_i x_4) + x_3 \exp(-t_i x_5)\Big),$$

with $t_i = 10(i-1)$ and data y_i. In this problem $m = 33$ and $n = 5$. The formulation of this problem is due to Osborne [23].

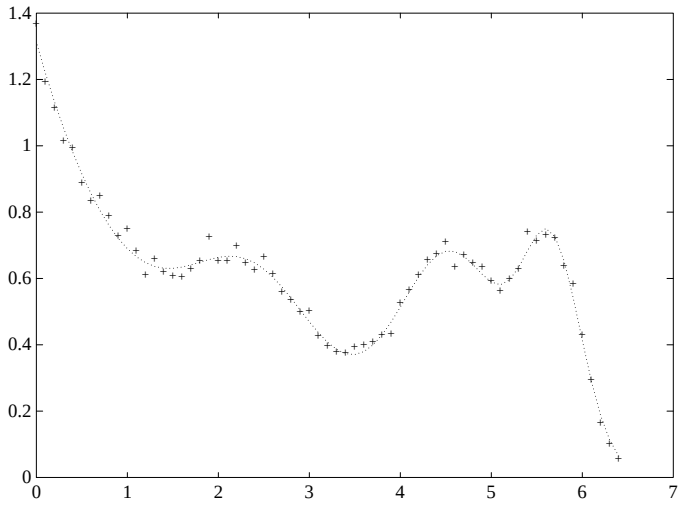

Figure 3.5: Exponential data fitting problem II

This problem is not difficult to solve from the standard starting point x_s and from the starting point $10x_s$, but underflows occur from the starting point $100x_s$. The bounds $-10 \leq x_j \leq 10$ for $1 \leq j \leq 5$ can be used to solve this problem. At the solution x^* we have

$$\|f(x^*)\| = 0.7392493 \times 10^{-2}.$$

A plot of the data and the model with the optimal parameters appears in Figure 3.4.

3.5 Exponential Data Fitting II

This is an exponential data fitting problem using data supplied by W. J. Caelli from the Research School of Physical Sciences of the Australian National University. The problem is of the form

$$f_i(x) = y_i - \Big(x_1 \exp(-t_i x_5) + x_2 \exp(-(t_i - x_9)^2 x_6) + x_3 \exp(-(t_i - x_{10})^2 x_7) + x_4 \exp(-(t_i - x_{11})^2 x_8)\Big),$$

with $t_i = (i-1)/10$ and data y_i. In this problem $m = 65$ and $n = 9$. The formulation of this problem is due to Osborne [23].

This problem is not difficult to solve from the standard starting point x_s, but underflows occur from other starting points. The bounds $0 \leq x_j \leq 10$ for $1 \leq j \leq 10$ can be used to solve this problem. At the solution x^* we have

$$\|f(x^*)\| = 0.2003440.$$

A plot of the data and the model with the optimal parameters appears in Figure 3.5.

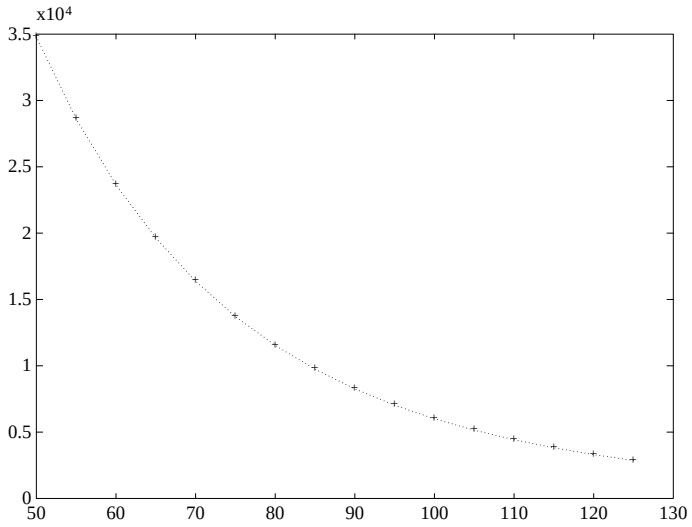

Figure 3.6: The thermistor resistance problem

3.6 Thermistor Resistance

The thermister resistance problem arises in the analysis of the resistance of a thermistor as a function of the temperature. The data was supplied by J. H. Hadley of the Shell Development Company. The problem is of the form

$$f_i(x) = x_1 \exp\left(\frac{x_2}{(t_i + x_3)}\right) - y_i,$$

with data y_i at the time points $t_i = 5 + 45i$ for $i = 1, \ldots, m$. In this problem $m = 16$ and $n = 3$. The formulation of this problem is due to Meyer [18].

This problem is difficult to solve even from the standard starting point x_s. At the solution x^* we have

$$\|f(x^*)\| = 9.377945 \ .$$

An algorithm can fail from other starting points because the dependence of this problem on t_i is lost for large values of x_3. In particular, if x_3 is sufficiently large, this problem reduces to a one-variable problem in the variable

$$z = x_1 \exp\left(\frac{x_2}{x_3}\right).$$

This situation can be avoided by imposing the bound $x_3 \leq 10^3$. This bound is fairly tight since at the solution, $x_3 = 345.22$.

A plot of the data and the model with the optimal parameters appears in Figure 3.6.

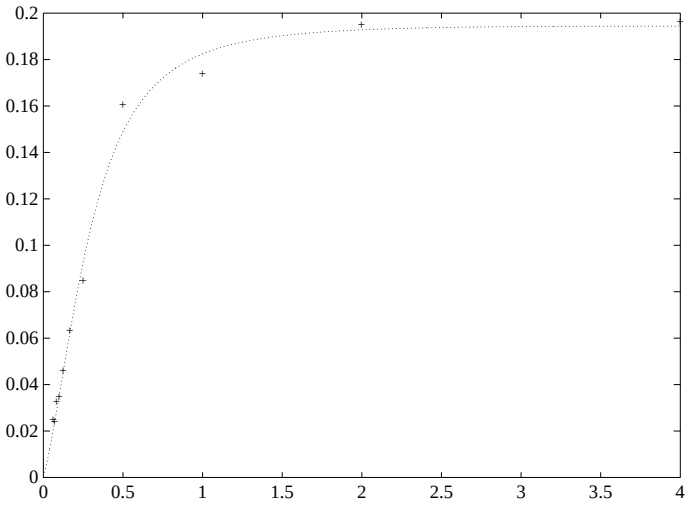

Figure 3.7: The enzyme problem

3.7 Analysis of an Enzyme Reaction

This problem arises in the analysis of the kinetic data for an enzyme reaction. The problem is of the form

$$f_i(x) = y_i - \frac{x_1(u_i^2 + u_i x_2)}{u_i^2 + u_i x_3 + x_4},$$

with data y_i and u_i. In this problem $m = 11$ and $n = 4$. This problem was formulated by Kowalik and Morrison [13].

This problem can be solved from the standard starting point x_s without difficulty. At the solution x^* we have

$$\|f(x^*)\| = 0.1753584 \times 10^{-1}.$$

From the starting point $10x_s$, algorithms may be attracted to a local minimizer at infinity with $x_2 = -14.075$. For this minimizer

$$\|f(x^*)\| = 0.3205219 \times 10^{-1}.$$

There are no bounds in this problem, but imposing the bounds $x_3 \geq 0$ and $x_4 \geq 0$ guarantees that the function is well defined, since $u_i \geq 0$ for all i. The local minimizer at infinity can be avoided by imposing the bounds $x_j \leq 100$ for $1 \leq j \leq 4$.

A plot of the data and the model with the optimal parameters appears in Figure 3.7.

3.8 Chebyshev Quadrature

The Chebyshev problem arises from the determination of the nodes of a quadrature formula with equal weights. The problem is of the form

$$f_i(x) = \frac{1}{n}\sum_{j=1}^{n} T_i(x_j) - \int_0^1 T_i(\xi)\, d\xi,$$

where T_i is the i-th Chebyshev polynomial shifted to the interval $[0, 1]$. In this problem any $m \geq n$ is allowed, but in the discussion below it is assumed that $m = n$. This problem was formulated by Fletcher [8].

The Chebyshev problem has a zero residual solution for $1 \leq n \leq 7$ and for $n = 9$. Note that the solution is not unique because any permutation of the variables also yields a solution. Thus, there are $n!$ distinct zero residual solutions. Such a zero residual solution can be obtained without difficulty from the standard starting point, but the problem becomes difficult to solve from the starting point $10x_s$ unless bounds are imposed. Since the nodes are required to be in the interval $[0, 1]$, the bounds $0 \leq x_j \leq 1$ for $1 \leq j \leq n$ are natural.

There seems to be a unique minimum of the least squares problem for $n = 8$ and $n = 11$. They are given by

$$\|f(x^*)\| = 0.5930324 \times 10^{-1}, \qquad n = 8,$$
$$\|f(x^*)\| = 0.5291277 \times 10^{-1}, \qquad n = 11.$$

We have found two local minima for $n = 10$. They are given by

$$\|f(x^*)\| = 0.6908483 \times 10^{-1}, \qquad \|f(x^*)\| = 0.8064710 \times 10^{-1}.$$

If an algorithm is started from the standard starting point, it will usually converge to the second minimum given above. There are multiple local minima for $n > 11$.

4 Minimization Problems

The problem of minimizing a function $f : \Re^n \to \Re$ subject to equality and inequality constraints can be expressed in the form

$$\min\{f(x) : c_l \leq c(x) \leq c_u\},$$

where $c : \Re^n \to \Re^p$ is the constraint function, and c_l and c_u are bounds. Equality constraints are obtained when components of c_l and c_u have the same value. Many of the problems in this section are bound-constrained problems; in this case $c(x) = x$.

4.1 Elastic-Plastic Torsion

The elastic plastic torsion problem arises from the determination of the stress field on an infinitely long cylindrical bar. The infinite-dimensional version of this problem is of the form

$$\min\{q(v) : v \in K\},$$

where $q : K \to \Re$ is the quadratic

$$q(v) = \tfrac{1}{2} \int_{\mathcal{D}} \|\nabla v(x)\|^2 \, dx - c \int_{\mathcal{D}} v(x) \, dx$$

for some constant c, and $\mathcal{D}$ is a bounded domain with smooth boundary. The convex set K is defined by

$$K = \{v \in H_0^1(\mathcal{D}) : |v(x)| \leq dist(x, \partial\mathcal{D}), \ x \in \mathcal{D}\},$$

where $dist(\cdot, \partial\mathcal{D})$ is the distance function to the boundary of $\mathcal{D}$, and $H_0^1(\mathcal{D})$ is the Hilbert space of all functions with compact support in $\mathcal{D}$ such that v and $\|\nabla v\|^2$ belong to $L^2(\mathcal{D})$. This formulation and the physical interpretation of the torsion problem are discussed, for example, in Glowinski [10, pp. 41–55].

A finite element approximation to the torsion problem is obtained by triangulating $\mathcal{D}$ and replacing the minimization of q over $H_0^1(\mathcal{D})$ by the minimization of q over the set of piecewise linear functions that satisfy the constraints specified by K. The finite element approximation thus gives rise to a finite-dimensional minimization problem whose variables are the values of the piecewise linear function at the vertices of the triangulation.

We develop a finite element approximation to a minimization problem with a quadratic q of the general form

$$q(v) = \tfrac{1}{2} \int_{\mathcal{D}} w_q(x) \|\nabla v(x)\|^2 \, dx - \int_{\mathcal{D}} w_l(x) v(x) \, dx, \tag{4.1}$$

where $w_q : \mathcal{D} \to \Re$ and $w_l : \mathcal{D} \to \Re$ are functions defined on the rectangle $\mathcal{D}$. In the torsion problem $w_q \equiv 1$ and $w_l \equiv c$.

Let $\mathcal{D} = (\xi_{1,l}, \xi_{1,u}) \times (\xi_{2,l}, \xi_{2,u})$ be a rectangle in $\Re^2$. Vertices $z_{i,j} \in \Re^2$ for a triangulation of $\mathcal{D}$ are obtained by choosing grid spacings h_x and h_y and defining grid points

$$z_{i,j} = (\xi_{1,l} + ih_x, \xi_{2,l} + jh_y), \qquad 0 \le i \le n_x + 1, \quad 0 \le j \le n_y + 1,$$

such that $z_{n_x+1,n_y+1} = (\xi_{1,u}, \xi_{2,u})$. The triangulation consists of triangular elements T_L with vertices at $z_{i,j}, z_{i+1,j}$, and $z_{i,j+1}$ and triangular elements T_U with vertices at $z_{i,j}, z_{i-1,j}$, and $z_{i,j-1}$.

A finite element approximation to the torsion problem is obtained by minimizing q over the space of piecewise linear functions v with values $v_{i,j}$ at $z_{i,j}$. The approximation to the integral

$$\int_{\mathcal{D}} w_q(x) \|\nabla v(x)\|^2 \, dx$$

over the element T_L is the quadratic $q^L_{i,j}$, where

$$q^L_{i,j}(v) = \mu_{i,j} \left\{ \left(\frac{v_{i+1,j} - v_{i,j}}{h_x} \right)^2 + \left(\frac{v_{i,j+1} - v_{i,j}}{h_y} \right)^2 \right\},$$

$$\mu_{i,j} = \frac{h_x h_y}{6} \left\{ w_q(z_{i,j}) + w_q(z_{i+1,j}) + w_q(z_{i,j+1}) \right\}.$$

Similarly, the approximation over the element T_U is the quadratic $q^U_{i,j}$, where

$$q^U_{i,j}(v) = \lambda_{i,j} \left\{ \left(\frac{v_{i-1,j} - v_{i,j}}{h_x} \right)^2 + \left(\frac{v_{i,j-1} - v_{i,j}}{h_y} \right)^2 \right\},$$

$$\lambda_{i,j} = \frac{h_x h_y}{6} \left\{ w_q(z_{i,j}) + w_q(z_{i-1,j}) + w_q(z_{i,j-1}) \right\}.$$

These calculations show that the finite element approximation to the quadratic (4.1) leads to a quadratic programming problem of the form

$$\min\{q(v) : v \in \Omega\}, \tag{4.2}$$

where q is the quadratic

$$q(v) = \frac{1}{2} \sum \left(q^L_{i,j}(v) + q^U_{i,j}(v) \right) - h_x h_y \sum w_l(z_{i,j}) v_{i,j}. \tag{4.3}$$

Note that in this formulation the quadratic $q^L_{i,j}$ is defined only when $0 \le i \le n_x$ and $0 \le j \le n_y$, while $q^U_{i,j}$ is defined when $1 \le i \le n_x + 1$ and $1 \le j \le n_y + 1$. Also note that for the torsion problem $w_q \equiv 1$ and $w_l \equiv c$ and that the feasible set Ω is

$$\Omega = \{v \in \Re^{n_x n_y} : |v_{i,j}| \le d_{i,j}\},$$

where $d_{i,j}$ is the value of $dist(\cdot, \partial\mathcal{D})$ at $z_{i,j}$.

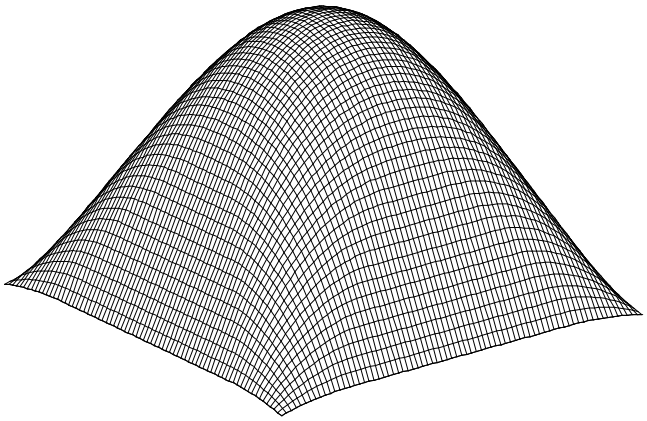

Figure 4.1: Torsion problem with $c = 5$

A plot of the solution to the finite-dimensional approximation to the torsion problem with $\mathcal{D} = (0,1) \times (0,1)$ and $c = 5$ appears in Figure 4.1. In general, the problem becomes easier to solve as c increases because then the linear term in q dominates. Numerical results for the elastic-plastic torsion problem are presented, for example, by O'Leary and Yang [22], Elliott and Ockendon [7, pp. 124–125], and Moré and Toraldo [19].

4.2 Pressure Distribution in a Journal Bearing

The journal bearing problem arises in the determination of the pressure distribution in a thin film of lubricant between two circular cylinders. The infinite-dimensional version of this problem is of the form

$$\min\{q(v) : v \in K\},$$

where $q : K \to \Re$ is the quadratic (4.1) with

$$w_q(\xi_1, \xi_2) = (1 + \epsilon \cos \xi_1)^3, \quad w_l(\xi_1, \xi_2) = \epsilon \sin \xi_1$$

for some constant ϵ in $(0,1)$, and $\mathcal{D} = (0, 2\pi) \times (0, 2b)$ for some constant $b > 0$. The convex set K is defined by

$$K = \{v \in H_0^1(\mathcal{D}) : v \geq 0 \text{ on } \mathcal{D}\}.$$

In the formulation of Cimatti [4], all functions in K were required to be periodic in the first argument with period 2π; in our formulation we have neglected the periodicity conditions.

A finite element approximation to the journal bearing problem is obtained as in the torsion problem. The result is a quadratic programming problem of the form (4.2), where q

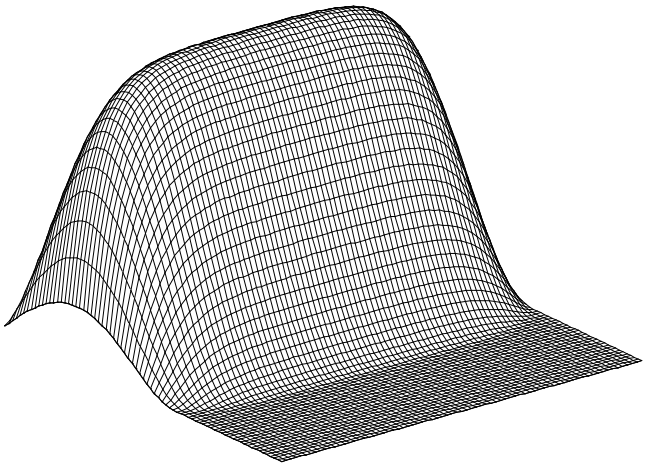

Figure 4.2: Journal bearing problem with $b = 10$ and $\epsilon = 0.1$

is the quadratic defined by (4.3). For the journal bearing problem $w_q(\xi_1, \xi_2) = (1+\epsilon\cos\xi_1)^3$ and $w_l(\xi_1, \xi_2) = \epsilon\sin\xi_1$, and the feasible set Ω is

$$\Omega = \{v \in \Re^{n_x n_y} : v_{i,j} \geq 0\}.$$

A plot of the solution to the finite-dimensional approximation to the journal bearing problem with $b = 10$ and $\epsilon = 0.1$ appears in Figure 4.2. This problem is harder to solve than the elastic-plastic torsion problem unless the problem is scaled so that the diagonal elements in the matrix that represents q are unity. Numerical results for the journal bearing problem are presented, for example, by Lin and Cryer [14], Cimatti and Menchi [5], and Moré and Toraldo [19].

4.3 Minimal Surfaces

The determination of the surface with minimal area and given boundary values in a convex domain $\mathcal{D}$ is an infinite-dimensional optimization problem of the form

$$\min\{f(v) : v \in K\},$$

where $f : K \to \Re$ is the functional

$$f(v) = \int_{\mathcal{D}} \left(1 + \|\nabla v(x)\|^2\right)^{1/2} dx,$$

and the set K is defined by

$$K = \left\{v \in H^1(\mathcal{D}) : v(x) = v_D(x) \text{ for } x \in \partial\mathcal{D}\right\}$$

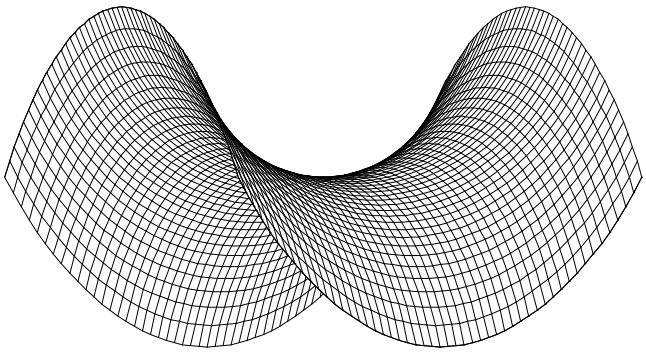

Figure 4.3: Enneper's minimal surface

for some boundary data function $v_D : \partial\mathcal{D} \to \Re$. The boundary function v_D uniquely defines the solution to the minimal surface problem.

An interesting minimal surface discovered by A. Enneper is obtained by defining v_D on $\mathcal{D} = (-\frac{1}{2}, \frac{1}{2}) \times (-\frac{1}{2}, \frac{1}{2})$ by

$$v_D(\xi_1, \xi_2) = u^2 - v^2,$$

where u and v are the unique solutions to the equations

$$\xi_1 = u + uv^2 - \frac{1}{3}u^3, \quad \xi_2 = -v - u^2 v + \frac{1}{3}v^3.$$

For more information on this minimal surface, see Nitsche [21, pp. 80–85]. A plot of this minimal surface appears in Figure 4.3.

A finite element approximation to the minimal surface problem is obtained by minimizing f over the space of piecewise linear functions v with values $v_{i,j}$ at $z_{i,j}$, where $z_{i,j} \in \Re^2$ are the vertices of a triangulation of $\mathcal{D}$ with grid spacings h_x and h_y. The values $v_{i,j}$ are obtained by solving the minimization problem

$$\min\{\sum \left(f_{i,j}^L(v) + f_{i,j}^U(v) \right) : v \in \Re^n\},$$

where the functions $f_{i,j}^L$ and $f_{i,j}^U$ are defined by

$$f_{i,j}^L(v) = \frac{h_x h_y}{2} \left\{ 1 + \left(\frac{v_{i+1,j} - v_{i,j}}{h_x} \right)^2 + \left(\frac{v_{i,j+1} - v_{i,j}}{h_y} \right)^2 \right\}^{1/2}$$

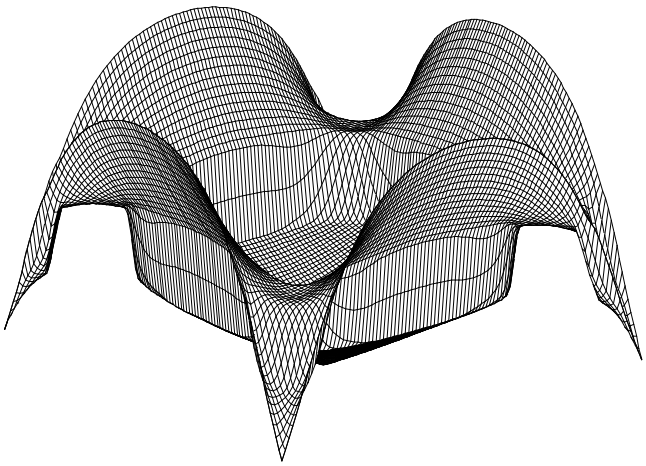

Figure 4.4: Norm $\|\nabla v\|$ for the stress field v in a design with composite materials

$$f_{i,j}^U(v) = \frac{h_x h_y}{2}\left\{1 + \left(\frac{v_{i-1,j} - v_{i,j}}{h_x}\right)^2 + \left(\frac{v_{i,j-1} - v_{i,j}}{h_y}\right)^2\right\}^{1/2}.$$

Note that in this formulation $f_{i,j}^L$ is defined only when $0 \le i \le n_x$ and $0 \le j \le n_y$, while $f_{i,j}^U$ is defined when $1 \le i \le n_x + 1$ and $1 \le j \le n_y + 1$.

4.4 Optimal Design with Composite Materials

This optimal design problem requires determining the placement of two elastic materials in the cross-section of a rod with maximal torsional rigidity. Our formulation follows the approach of Goodman, Kohn, and Reyna [11].

Let $\mathcal{D}$ in $\Re^2$ be a bounded domain, and let $w < |\mathcal{D}|$, where $|\mathcal{D}|$ denotes the area of $\mathcal{D}$. The solution of the optimal design problem is a subset Ω of $\mathcal{D}$ that solves the problem

$$\min\{\mathcal{F}(v,\Omega) : v \in H_0^1(\mathcal{D}),\ |\Omega| = w\}$$

where

$$\mathcal{F}(v,\Omega) = \int_{\mathcal{D}} \left\{\tfrac{1}{2}\mu(x)\|\nabla v(x)\|^2 + v(x)\right\} dx,$$

and

$$\mu(x) = \mu_1,\ x \in \Omega, \quad \mu(x) = \mu_2,\ x \notin \Omega.$$

The reciprocals of the constants μ_1 and μ_2 are the shear moduli of the elastic materials in the rod. We assume that $\mu_1 < \mu_2$.

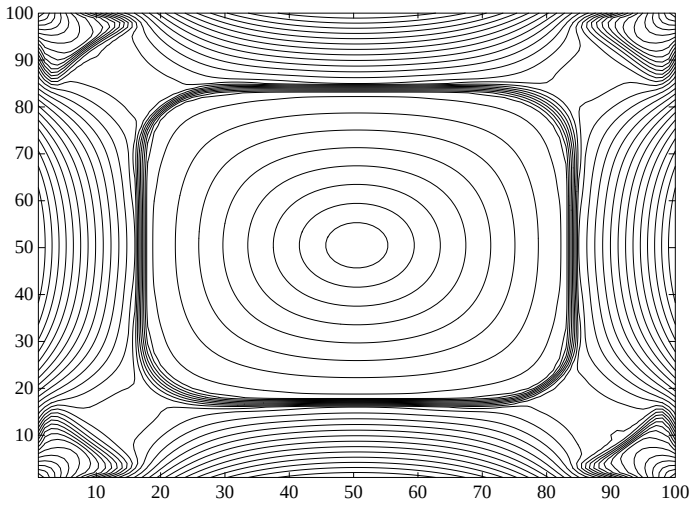

Figure 4.5: Contours of $\|\nabla v\|$ for the stress field v in a design with composite materials

Goodman, Kohn, and Reyna [11] formulate the optimal design problem in terms of a family of problems of the form

$$\min\{f_\lambda(v) : v \in H_0^1(\mathcal{D})\},$$

where $f_\lambda : H_0^1(\mathcal{D}) \to \Re$ is the functional

$$f_\lambda(v) = \int_{\mathcal{D}} \Big\{ \psi_\lambda \left(\|\nabla v(x)\| \right) + v(x) \Big\} \, dx$$

and $\psi_\lambda : \Re \to \Re$ is a piecewise quadratic. In this formulation λ is a Lagrange multiplier associated with the optimal design problem, and the piecewise quadratic $\psi_\lambda : \Re \to \Re$ is of the form

$$\psi_\lambda(t) = \begin{cases} \frac{1}{2}\mu_2 t^2, & 0 \le t \le t_1, \\ \mu_2 t_1 (t - \frac{1}{2} t_1), & t_1 \le t \le t_2, \\ \frac{1}{2}\mu_1 (t^2 - t_2^2) + \mu_2 t_1 (t_2 - \frac{1}{2} t_1), & t_2 \le t, \end{cases}$$

with the breakpoints t_1 and t_2 defined by

$$t_1 = \left(2\lambda \frac{\mu_1}{\mu_2} \right)^{\frac{1}{2}}, \qquad t_2 = \left(2\lambda \frac{\mu_2}{\mu_1} \right)^{\frac{1}{2}}.$$

The definition of the breakpoints implies that $\mu_1 t_2 = \mu_2 t_1$, and thus ψ is continuously differentiable. The solution of the optimum design requires determining a λ that maximizes the mapping $\Phi : \Re \to \Re$ defined by

$$\Phi(\lambda) = \phi(\lambda) + [(\mu_1 - \mu_2) w] \lambda,$$

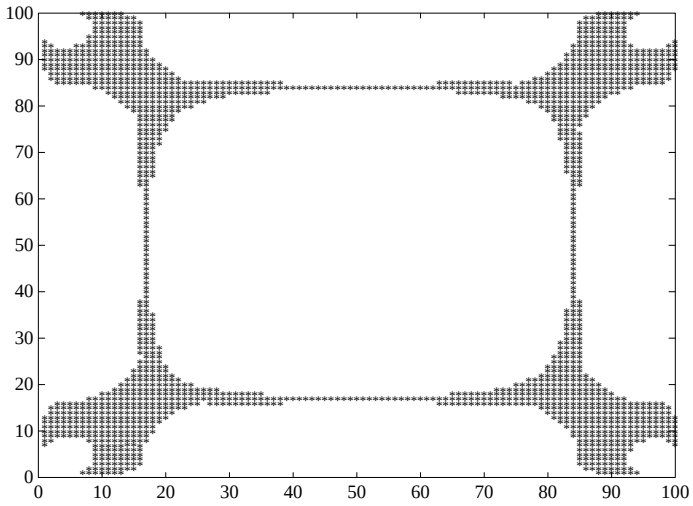

Figure 4.6: Region of homogenization in a design with composite materials ($n = 10^4$)

where $\phi(\lambda)$ is the minimum value of f_λ. Goodman, Kohn, and Reyna [11] describe how the solution of the maximization problem defined by Φ can be used to generate a minimizing sequence for the optimal design problem.

In the sequel we consider only the problem of minimizing f_λ for a fixed value of λ. A finite element approximation to this problem is obtained by minimizing f_λ over the space of piecewise linear functions v with values $v_{i,j}$ at $z_{i,j}$, where $z_{i,j} \in \Re^2$ are the vertices of a triangulation of $\mathcal{D}$ with grid spacings h_x and h_y. The values $v_{i,j}$ are obtained by solving the minimization problem

$$\min\{\sum \left(f^L_{i,j}(v) + f^U_{i,j}(v) + v_{i,j} \right) : v \in \Re^n\},$$

where the functions $f^L_{i,j}$ and $f^U_{i,j}$ are defined by

$$f^L_{i,j}(v) = \frac{h_x h_y}{2} \psi_\lambda \left(d^+_{i,j}(v) \right), \quad f^U_{i,j}(v) = \frac{h_x h_y}{2} \psi_\lambda \left(d^-_{i,j}(v) \right)$$

with

$$d^\pm_{i,j}(v) = \left\{ \left(\frac{v_{i\pm1,j} - v_{i,j}}{h_x} \right)^2 + \left(\frac{v_{i,j\pm1} - v_{i,j}}{h_y} \right)^2 \right\}^{1/2}$$

Note that in this formulation $f^L_{i,j}$ is defined only when $0 \le i \le n_x$ and $0 \le j \le n_y$, while $f^U_{i,j}$ is defined when $1 \le i \le n_x + 1$ and $1 \le j \le n_y + 1$.

In our numerical results we used $\mu_1 = 1$ and $\mu_2 = 2$, so that $t_1^2 = \lambda$. A plot of the norm $\|\nabla v\|$ of the gradient of the stress field v with $\mathcal{D} = (0,1) \times (0,1)$ and $t_1^2 = 0.008$ appears

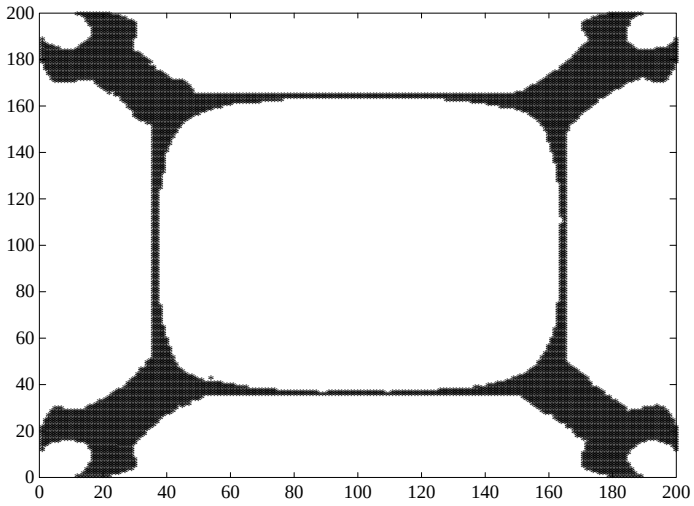

Figure 4.7: Region of homogenization in a design with composite materials ($n = 4 \times 10^4$)

in Figure 4.4. Figure 4.5 is the contour plot for this surface. In both figures we have used $n_x = n_y = 100$ so that $n = 10^4$.

Figures 4.4 and 4.5 show that $\|\nabla v\|$ is changing slowly in the center of $\mathcal{D}$, where $\|\nabla v(x)\| \leq t_1$. On the other hand, the gradient changes quite rapidly in the region where $t_1 \leq \|\nabla v(x)\| \leq t_2$. We are not even guaranteed a continuous gradient ∇v in this region. Thus, approximation by piecewise linear elements seems to be fully justified in this problem.

The rod has the material with greater shear modulus $1/\mu_1$ where the shear $\|\nabla v(x)\| > t_2$, and the weaker material where $\|\nabla v(x)\| < t_1$. Figure 4.4 shows that in the optimal design, the weaker material is placed in the center and corners of the rod.

The region where $t_1 \leq \|\nabla v(x)\| \leq t_2$ is the homogenized region. The geometry and placement of the region of homogenization are of interest in the optimal design. It is known, for example, that in general the boundary of this region is not smooth. The plots of this region in Figures 4.6 and 4.7 indicate the unusual nature of this region.

The contour plot in Figure 4.5 and the plots of the region of homogenization in Figures 4.6 and 4.7 are similar to those obtained by Goodman, Kohn, and Reyna [11]. Note, however, that in these plots we used $t_1^2 = 0.008$, while Goodman, Kohn, and Reyna [11] used $t_1^2 = 0.002$. Another difference is that the homogenized region in these plots is connected, while this is not the case in the results of Goodman, Kohn, and Reyna [11].

4.5 Inhomogeneous Superconductors

This problem arises in the solution of the Ginzburg-Landau equations for inhomogeneous superconductors in the absence of a magnetic field. The one-dimensional system under consideration consists of alternating layers of lead and tin. Our formulation is based on the work of Garner and Benedek [9].

The optimization problem is to minimize the Gibbs free energy as a function of the temperature. The infinite-dimensional version of this problem is of the form

$$\min\{f(v) : v(-d) = v(d),\ v \in C^1[-d,d]\},$$

where $2d$ is the width of the material, and f is the Gibbs free energy function. In this problem

$$f(v) = \frac{1}{2d}\int_{-d}^{d}\left\{\alpha(\xi)|v(\xi)|^2 + \tfrac{1}{2}\beta(\xi)|v(\xi)|^4 + \frac{\hbar}{4m}|v'(\xi)|^2\right\}\ d\xi,$$

the functions α and β are piecewise constant for a fixed value of the temperature, $\hbar$ is Planck's constant, and m is the mass of the electron.

The functions α and β are constant in the intervals that correspond to the lead and the tin. Since in this problem the lead in the material corresponds to the interval $[-d_s, d_s]$ and tin in the remaining part of the interval $[-d,d]$, the function α is defined by

$$\alpha(\xi) = \begin{cases} \alpha_N, & -d \le \xi \le -d_S \\ \alpha_S, & -d_S < \xi \le d_S \\ \alpha_N, & d_S < \xi \le d \end{cases}.$$

Similarly, the function β is defined by

$$\beta(\xi) = \begin{cases} \beta_N, & -d \le \xi \le -d_S \\ \beta_S, & -d_S < \xi \le d_S \\ \beta_N, & d_S < \xi \le d \end{cases}.$$

The constants α_S and α_N are negative, but β_S and β_N are positive.

A finite element approximation to the superconductivity problem is obtained by minimizing f over the space of piecewise linear functions v with values v_i at t_i, where

$$-d = t_1 < t_2 < \ldots < t_n < t_{n+1} = d.$$

We assume that there are indices n_1 and n_2 such that $t_{n_1} = -d_S$ and $t_{n_2} = d_S$, where $1 < n_1 < n_2 < n$. This guarantees that the t_i do not straddle a point of discontinuity of the functions α and β. The values v_i are obtained by solving the minimization problem

$$\min\{\frac{1}{2d}\sum_{i=1}^{n} f_i(v) : v \in \Re^n\},$$

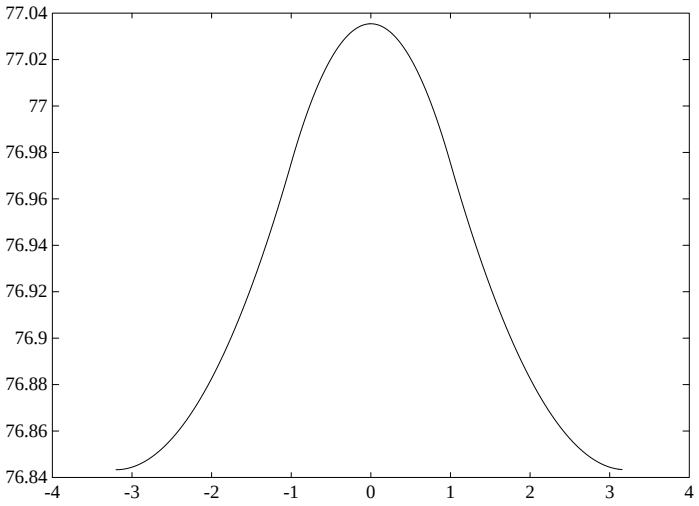

Figure 4.8: Superconductivity problem

where

$$f_i(v) = h_i \left\{ \frac{\alpha_i}{3} \frac{v_{i+1}^3 - v_i^3}{v_{i+1} - v_i} + \frac{\beta_i}{5} \frac{v_{i+1}^5 - v_i^5}{v_{i+1} - v_i} + \frac{\hbar}{4m} \left(\frac{v_{i+1} - v_i}{h_i} \right)^2 \right\},$$

with $h_i = t_{i+1} - t_i$ the length of the i-th interval, and the constants α_i and β_i the values of the functions α and β in the interval $[t_i, t_{i+1}]$. The constraint that $v(-d) = v(d)$ is taken into account by requiring that $v_{n+1} = v_1$.

References

[1] U. Ascher, *Solving boundary-value problems with a spline-collocation code*, J. Comput. Phy., 34 (1980), pp. 401–413.

[2] U. M. Ascher, R. M. M. Mattheij, and R. D. Russell, *Numerical solution of boundary value problems for ordinary differential equations*, Prentice Hall, 1988.

[3] G. E. P. Box, W. G. Hunter, J. F. MacGregor, and J. Erjavec, *Some problems associated with the analysis of multiresponse data*, Technometrics, 15 (1973), pp. 33–51.

[4] G. Cimatti, *On a problem of the theory of lubrication governed by a variational inequality*, Appl. Math. Optim., 3 (1977), pp. 227–242.

[5] G. Cimatti and O. Menchi, *On the numerical solution of a variational inequality connected with the hydrodynamic lubrication of a complete journal bearing*, Calcolo, 15 (1978), pp. 249–258.

[6] J. E. Dennis, D. M. Gay, and P. A. Vu, *A new nonlinear equations test problem*, Report 83-16, Rice University, Houston, Texas, 1983. Revised January 1986.

[7] C. M. Elliott and J. R. Ockendon, *Weak and Variational Methods for Moving Boundary Problems*, vol. 59 of Research Notes in Mathematics, Pittman, 1982.

[8] R. Fletcher, *Function minimization without derivatives – A review*, Comput. J., 8 (1965), pp. 33–41.

[9] J. Garner and R. Benedek, *Solution of Ginzburg-Landau equations for inhomogeneous superconductors by nonlinear optimization*, Phys. Rev. B, 42 (1990), pp. 376–385.

[10] R. Glowinski, *Numerical Methods for Nonlinear Variational Problems*, Springer-Verlag, 1984.

[11] J. Goodman, R. Kohn, and L. Reyna, *Numerical study of a relaxed variational problem from optimal design*, Comput. Methods Appl. Mech. Engrg., 57 (1986), pp. 107–127.

[12] C. L. Huang, *Applications of quasilinearization technique to the vertical channel and heat convection*, Int. J. Nonlinear Mech., 13 (1978), pp. 55–60.

[13] J. Kowalik and J. F. Morrison, *Analysis of kinetic data for allosteric enzyme reactions as a nonlinear regression problem*, Math. Biosci., 2 (1968), pp. 57–66.

[14] Y. Lin and C. W. Cryer, *An alternating direction implicit algorithm for the solution of linear complementarity problems arising from free boundary problems*, Appl. Math. Optim., 13 (1985), pp. 1–17.

[15] J. N. Lyness, *When not to use an automatic quadrature routine*, SIAM Rev., 25 (1983), pp. 63–87.

[16] J. B. McLeod and S. V. Parter, *On the flow between two counter-rotating infinite plane disks*, Arch. Rat. Mech. Anal, 54 (1974), pp. 301–327.

[17] K. Meintjes and A. P. Morgan, *Chemical equilibrium systems as numerical test problems*, ACM Trans. Math. Software, 16 (1990), pp. 143–151.

[18] R. R. Meyer, *Theoretical and computational aspects of nonlinear regression*, in Nonlinear Programming, J. B. Rosen, O. L. Mangasarian, and K. Ritter, eds., Academic Press, 1970.

[19] J. J. Moré and G. Toraldo, *On the solution of large quadratic programming problems with bound constraints*, SIAM J. Optimization, 1 (1991), pp. 93–113.

[20] C. V. Nelson and B. C. Hodgkin, *Determination of magnitudes, directions and locations of two independent dipoles in a circular conducting region from boundary potential measurements*, IEEE Trans. Biomed. Eng., 28 (1981), pp. 817–823.

[21] J. C. C. Nitsche, *Lectures on Minimal Surfaces*, vol. 1, Cambridge University Press, 1989.

[22] D. P. O'Leary and W. H. Yang, *Elastoplastic torsion by quadratic programming*, Comput. Methods Appl. Mech. Engrg., 16 (1978), pp. 361–368.

[23] M. R. Osborne, *Some aspects of non-linear least squares calculations*, in Numerical Methods for Nonlinear Optimization, F. A. Lootsma, ed., Academic Press, 1972.

[24] S. V. Parter, *On the swirling flow between rotating coaxial disks: A survey*, in Theory and Applications of Singular Perturbations, W. Eckhaus and E. M. de Jager, eds., vol. 942 of Lecture Notes in Mathematics, Springer Verlag, 1982, pp. 258–280.

[25] I.-B. Tjoa and L. T. Biegler, *Simultaneous solution and optimization strategies for parameter estimation of differential-algebraic equations systems*, Ind. Eng. Chem. Res., 30 (1991), pp. 376–385.